

Scattering of Electrons and Positrons by Cobalt and Bismuth: Calculations

ROBERT HERMAN AND B. C. CLARK

General Motors Research Laboratories, Warren, Michigan

AND

D. G. RAVENHALL*

University of Illinois, Urbana, Illinois

(Received 13 May 1963)

Partial-wave calculations of electron and positron scattering by cobalt and bismuth are presented, and compared with the experimental results of Goldemberg, Pine, and Yount. A physical description of the scattering process is given which throws light on the general behavior of the calculational cross sections. Their dependence on incident energy, and on the assumed nuclear charge distribution is discussed.

I. INTRODUCTION

THE purpose of this paper is to present partial-wave calculations of electron and positron scattering by cobalt and bismuth to be compared with the experiments of Goldemberg, Pine, and Yount.¹ The calculations are based on the information already obtained about the nuclear distribution from the earlier electron scattering work of Hahn, Ravenhall, and Hofstadter.² The close agreement with the GPY experiments is a confirmation of the basic assumption that, under the conditions of these experiments, electrons and positrons interact only with the Coulomb field of the nuclear charge distribution. The calculations are extensive enough to enable us to examine the sensitivity of this ratio type of experiment to the assumed nuclear charge distribution, and to the energy of the incident particles.

A comparison is also made with the small-angle approximation of Drell and Pratt.³ Close agreement at the smallest angles, for cobalt, serves as an independent check of our computational method, while departures at larger angles, and for bismuth, display the higher Born approximation contributions which their treatment leaves out. Our calculations seem to be in qualitative agreement with those of Rawitscher and Fischer,⁴ although since the energy and elements considered by them are different from those of the GPY experiment, a detailed comparison has not been made. The second Born approximation calculations of Budini and Furlan⁵ seem to be in agreement with those of Drell and Pratt, but for the same reason we have not been able to compare them in detail.

Section II describes our calculational method. The particular results obtained are presented in Sec. III. A physical description of them, which throws light on their various features, is given in Sec. IV. Section V comments on the comparison with the GPY experiments.

* Supported in part by the U. S. National Science Foundation.

¹ J. Goldemberg, J. Pine, and D. Yount, preceding paper, *Phys. Rev.* **132**, 406 (1963), referred to as GPY.

² B. Hahn, D. G. Ravenhall, and R. Hofstadter, *Phys. Rev.* **101**, 1131 (1956), henceforth referred to as HRH.

³ S. D. Drell and R. H. Pratt, *Phys. Rev.* **125**, 1394 (1962).

⁴ G. H. Rawitscher and C. R. Fischer, *Phys. Rev.* **122**, 1330 (1961).

⁵ P. Budini and G. Furlan, *Nuovo Cimento* **13**, 790 (1959).

II. THEORY AND METHOD

In the Dirac equation which describes the motion of the electron or positron, the nucleus is represented by the Coulomb potential of a static, spherically symmetric charge distribution. The scattering amplitude is obtained by a numerical partial-wave analysis which follows closely the methods described by Yennie, Ravenhall, and Wilson,⁶ and we shall refer the reader to that paper for equations and formulas. Briefly, the procedure is as follows. Phase shifts measuring the effect of the finite charge distribution, obtained by numerical integration of the radial Dirac equation, are added to the phases for Coulomb scattering by a point charge. The total phase shifts are then inserted in the Legendre series for the scattering amplitude. The differential cross section for positrons is obtained with exactly the same procedure as that used for electrons, the only change being that the parameter $\gamma = (Ze^2/\hbar c)$, which characterizes the electron-nucleus Coulomb interaction, is replaced by $-\gamma$. Having obtained the electron (positron) differential cross section $d\sigma_e/d\Omega = \sigma_-$ ($d\sigma_p/d\Omega = \sigma_+$), we then calculate the quantity R measured by Goldemberg, Pine, and Yount:

$$R(\theta) = (\sigma_- - \sigma_+) / (\sigma_- + \sigma_+).$$

In the energy region covered by these calculations, where $E_0 \gg mc^2$, the dominant quantity of dimensions of length is $\lambda = \hbar c / E_0$, the electron reduced Compton wavelength. There is an implicit dependence of cross sections on λ , or $k = \lambda^{-1}$, because in the Dirac equation the length parameters c and z of the charge distributions occur in the dimensionless combinations kc , kz . Apart from a smooth kinematic factor, the angular variation of differential cross sections thus depends on kc and kz . The only explicit dependence on λ is as a multiplicative factor in the scattering amplitude. For a given kc , etc., the effect of the actual value of k is to change the cross section at all angles by a factor $\lambda^2 = k^{-2}$. Because of the ratio form of R , this latter dependence on k disappears. R depends only on kc and kz , and, in general, only on the values of the length parameters in units of λ .

⁶ D. R. Yennie, D. G. Ravenhall, and R. Wilson, *Phys. Rev.* **95**, 500 (1954).

TABLE I. Some numerical values of differential cross sections and of R , for the Fermi shape at 300 MeV, for comparison with other calculations. Each case is specified completely by the following parameter values: cobalt, $\gamma = Ze^2/\hbar c = \pm 0.1970$, $kc = 6.37$, $kz = 0.796$; bismuth, $\gamma = \pm 0.6056$, $kc = 10.10$, $kz = 0.8558$; $\hbar = 1.5204\text{F}^{-1}$. σ_- and σ_+ are the cross sections for electrons and positrons, respectively, in mb/sr, the number in parenthesis being the power of ten multiplying the quoted decimal. They are not folded over angles.

θ°	Cobalt			Bismuth		
	σ_-	σ_+	R	σ_-	σ_+	R
10	0.537(3)	0.521(3)	0.015	0.448(4)	0.437(4)	0.012
20	0.110(2)	0.120(2)	-0.044	0.296(2)	0.446(2)	-0.202
40	0.546(-2)	0.555(-2)	-0.008	0.298(-1)	0.666(-1)	-0.382
60	0.270(-3)	0.442(-3)	-0.241	0.250(-3)	0.754(-3)	-0.502
80	0.135(-4)	0.339(-5)	0.599	0.610(-5)	0.241(-4)	-0.596

A discussion of the accuracy of our present results, the output of a FORTRAN program written for the IBM-7090 computer at the General Motors Research Laboratories, will be presented in a forthcoming paper.⁷ The special additional feature required for the present results concerns the numerical summing of the Legendre series. The reduction method employed to make this series converge more rapidly⁸ yields a new series whose coefficients are approximately the second differences of the original coefficients. After using this reduction method three times successively, there is a considerable loss of numerical significance in the coefficients of the final series. The smaller the scattering angle, the more slowly the Legendre function $P_n(\cos\theta)$ decreases with n . More terms of the scattering amplitude series are needed, and this loss of significance becomes a limiting factor. An elegant remedy for this problem would be to separate from the total amplitude the nonrelativistic Coulomb point-charge amplitude whose analytic sum is well known. It is the most singular part of the scattering amplitude for $\theta \rightarrow 0$, and consequently, is responsible for the least convergent part of the Legendre series. The remaining part, which is still singular as $\theta \rightarrow 0$, can also be summed analytically, in an appropriate way which

TABLE II. Comparison of results for uniform charge distributions with the approximation of Drell and Pratt.^a Their result for R , called R_{DP} , was calculated from Eq. (17) of Ref. 3. The independent variable of their calculation, $x = \Delta a$, has the following relation to quantities used in the present paper: $x = (3/5)^{1/2} 2kc \sin^2\theta$. The two uniform shapes are: cobalt, $\gamma (= Ze^2/\hbar c) = 0.1970$, $kc = 6.37$; bismuth, $\gamma = 0.6056$, $kc = 10.10$.

x	θ°	Cobalt		Bismuth		
		R	R_{DP}	θ°	R	R_{DP}
0.5	5.81	0.191	0.191	3.66	0.0345	0.0371
1.0	11.63	0.0169	0.0161	7.33	0.0411	0.0311
1.5	17.49	-0.0076	-0.0100	11.00	0.0080	-0.0194
2.0	23.39	-0.0618	-0.0676	14.69	-0.0630	-0.1311
2.5	29.35	-0.1670	-0.1876	18.39	-0.1622	-0.3638
3.0	35.40	-0.3689	-0.5315	22.11	-0.2189	-1.0304

^a See Ref. 3.

⁷ D. G. Ravenhall, R. Herman, and B. C. Clark (unpublished).

⁸ See Ref. 6, Eq. (47) and the material following it.

is reliable for $\theta \rightarrow 0$.⁹ Because of the relative simplicity with which double precision arithmetic may be done in FORTRAN on the IBM-7090 computer, we chose the inelegant alternative of obtaining and summing the relativistic Coulomb point-charge amplitude numerically with double precision. With sixteen digits available, the loss of significance does not jeopardize the precision of the sum until the scattering angles become smaller than around 5° . The contribution to the amplitude from the finite extent of the charge distribution—the nuclear phase shift part—is not singular at $\theta \rightarrow 0$. It is calculated in single precision, and the result added to the point-scattering amplitude. The results of this method agree well with those entirely in single precision at angles beyond about 25° .

To allow a check with later calculations, we have presented in Table I some sample numerical results, for the Fermi distributions considered in the next section. A comparison of the exact partial-wave results for the uniform distribution with the second-Born approximation expressions derived by Drell and Pratt³ is made in Table II. Their treatment is exact in the limit of small

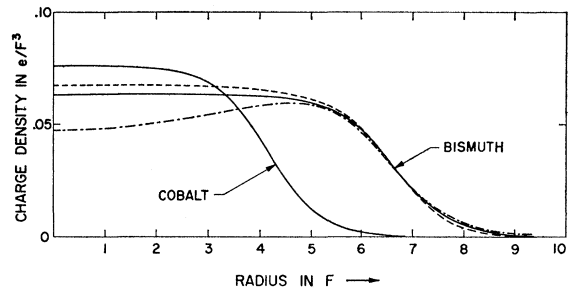


FIG. 1. Charge distribution for bismuth and cobalt. The solid line for bismuth is the Fermi shape (1), $c = 6.64\text{F}$, $z = 0.56\text{F}$; the dashed line is the modified Gaussian shape (2), $c = 6.58\text{F}$, $z = 2.76\text{F}$; and the dash-line is the parabolic Fermi shape (3), $c = 6.32\text{F}$, $z = 0.65\text{F}$, $w = 0.64$. The cobalt curve is the Fermi shape (1), $c = 4.19\text{F}$, $z = 0.52\text{F}$.

angles, and the agreement, for cobalt, at the two smallest angles is a useful check on our numerical work. The progressive difference at the larger angles shows the presence of the higher Born terms neglected in their calculation. In bismuth, it seems that the agreement with their approximation must occur at angles too small for our code to handle. This is presumably due to the larger value of Z .

III. CALCULATIONS

To describe the static nuclear charge distribution we have employed the following three shapes. They were used in the electron-scattering analysis of HRH, and

⁹ The corresponding treatment for the Klein-Gordon equation has been formulated by J. H. Hetherington, Ph.D. thesis, University of Illinois, 1960 (unpublished); J. H. Hetherington, J. Math. Phys. 4, 357 (1963).

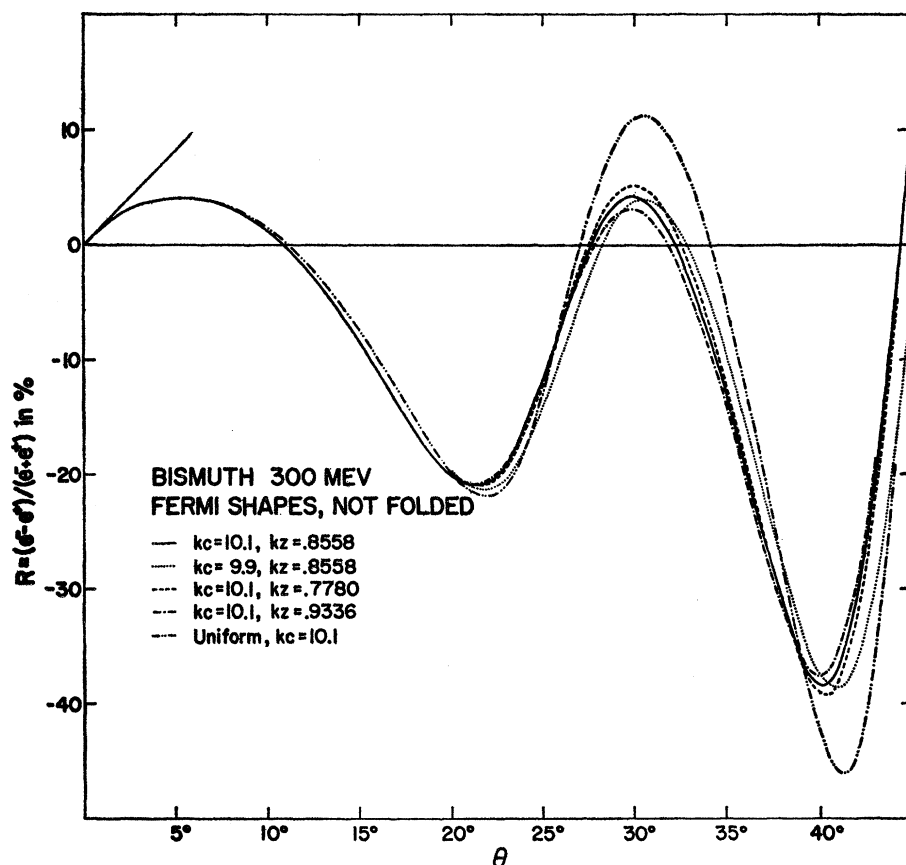


FIG. 2. Plots of the quantity R versus θ , for various Fermi shapes in bismuth. As is described in Sec. 2, R is a function only of kc and kz . Besides the central value $kc=10.1$, $kz=0.8558$, there are curves for kc decreased by 2%, to illustrate the sensitivity to the charge distribution parameters. For comparison there is also included the curve for the uniform shape, $kc=10.1$. The tangent at $\theta=0^\circ$ is what is obtained with a point charge (see Ref. 13).

are expressed in the notation of that paper²:

Fermi:

$$\rho(r) = \rho_1 \{ \exp[(r-c_1)/z_1] + 1 \}^{-1};$$

Modified Gaussian:

$$\rho(r) = \rho_2 \{ \exp[(r^2 - c_2^2)/z_2^2] + 1 \}^{-1};$$

Parabolic Fermi:

$$\rho(r) = \rho_3 [1 + (wr^2/c^2)] \{ \exp[(r-c_3)/z_3] + 1 \}^{-1}.$$

The charge distributions represented by these expressions, for particular parameter values used in this paper, are illustrated in Fig. 1. For the first two shapes, which are constant in the interior and have a diffuse edge, the parameter c is the distance to the half-point, the radius where $\rho(r)$ is half of its central value. The parameter z determines the surface thickness, but its relationship to t , the 90 to 10% thickness, is different for each shape: Fermi, $t=4.40 z_1$; modified Gaussian, $t \approx 2.20 z_2^2/c$. Because of the extra factor (wr^2/c^2) in the parabolic Fermi shape, the physical meaning of c and z for it are not precisely the same as with the Fermi shape, but qualitatively they have the same effect. The additional parameter w permits a smooth variation of the charge density in the inner region.

A useful theoretical reference point is provided by the uniform charge distribution, for which the density is

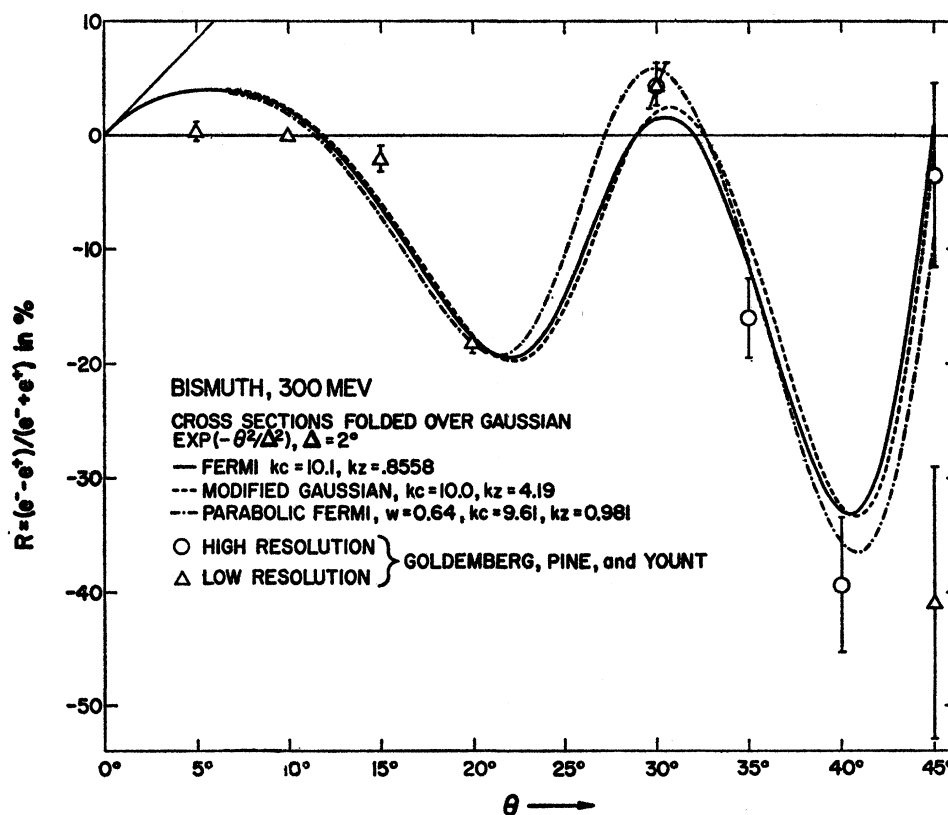
constant, but which has a sharp edge. Such a shape results from allowing z to approach zero in the Fermi or modified Gaussian shapes.

The results of the HRH analysis of relative differential cross sections for electron scattering were that the parameters c and t could be determined to about $\pm 2\%$ and $\pm 10\%$, respectively. It was well known previously, of course, that t was significantly greater than zero, i.e., that no uniform shape could yield agreement with experiment.¹⁰ In a detailed analysis of one element, gold (^{197}Au), shapes like the Fermi or modified Gaussian were found to be about equally acceptable, provided that in each case c and z were chosen appropriately. An approximately shape-independent surface thickness was found in the 90 to 10% distance t . For the parabolic Fermi shape the "best" value of w was 0.64, but acceptable values included $w=0$. It is against this background of knowledge that we discuss the information available with the electron-positron ratio experiments.

For bismuth and cobalt, the HRH analysis used only the Fermi shape. The quoted values of the parameters were: bismuth, $c=6.47$ F, $t=2.7$ F; cobalt, $c=4.09$ F, $t=2.5$ F. At the energy of the GPY ratio experiments,

¹⁰ See, for example, Ref. 6. A complete bibliography is contained in R. Hofstadter's *Nuclear and Nucleon Structure* (W. A. Benjamin, Inc., New York, 1963).

FIG. 3. A comparison of the quantity R expected from the electron scattering analysis (see Ref. 2) and the GPY experiments (see Ref. 1) for bismuth. With the central Fermi curve of Fig. 2 are shown the corresponding curves for the modified Gaussian and parabolic Fermi shapes, with the parameter values indicated. These curves have been folded over angles; see Fig. 4. Thus, the Fermi curve is not the same as the corresponding one in Fig. 2.



302 MeV (corresponding to $k=1.53 \text{ F}^{-1}$), the central parameter values of our calculation should thus be: bismuth, $kc=9.90, kz=0.94$; cobalt, $kc=6.26, kz=0.87$. More recent studies of electron scattering by Crannell *et al.*,¹¹ who measured absolute values of differential cross sections, have suggested that the value $t=2.7 \text{ F}$ for bismuth is too large, and should be somewhat reduced. Another set of values obtained in HRH at a different energy¹² also included a lower value of t in bismuth. Also, for historical reasons, our first ratio calculations assumed an energy of 307 MeV. Consequently, our central parameter values for the Fermi shape are not exactly those quoted above, but are bismuth, $kc=10.1, kz=0.8558$; cobalt, $kc=6.37, kz=0.796$. (These dimensionless numbers, together with $\gamma=Ze^2/\hbar c=0.1970$, cobalt; $\gamma=0.6056$, bismuth, specify our calculation completely.) In any case the regions within the quoted errors of the HRH values are covered adequately.

Figure 2 shows curves of R versus θ in bismuth, for the Fermi shape just quoted. To explore the sensitivity to variation of parameters, curves are included for kc decreased by 2% and for kz increased and decreased

by 10%. We include also the case of a uniform distribution, to exhibit the limit of zero surface thickness.

The ratio curves for modified Gaussian and parabolic Fermi distributions cannot be predicted with complete confidence, since the HRH fitting to the electron-scattering experiments was not done with these shapes. We have estimated the parameters c, z (and w for the parabolic Fermi shape) from their known values for gold, scaling c and z in the way indicated by the Fermi shape. The results are given in Fig. 3, together with the experimental data of GPY. The fact that over the range of recoil momenta covered by the electron experiments, which at 300 MeV correspond to angles between 20° and 55° , the ratios for the three shapes we have used are closely similar suggests that the above estimates are reasonably close. Whether or not it would be possible to bring the parabolic Fermi ratio into closer agreement with the other two by adjusting its c and z parameters we have not investigated in detail. Such an adjustment should be accompanied by a reanalysis of the electron scattering experiments, and this we have deferred until new results are available.

The curves of Fig. 3 include the small, but not inappreciable, effect of the finite angular resolution of the experiments. In a manner described in Ref. 2, the electron and positron cross sections have been folded over angles separately, with for convenience the functional form $\exp[-(\theta-\theta')^2/\Delta^2]$, where Δ has been

¹¹ H. Crannell, R. Helm, H. Kendall, J. Oeser, and M. Yearian, *Phys. Rev.* **121**, 283 (1961).

¹² See p. 1139 of Ref. 2.

¹³ See, for example, N. F. Mott and H. S. W. Massey, *The Theory of Atomic Collisions*, 2nd ed. (Oxford University Press, London, 1952), p. 82.

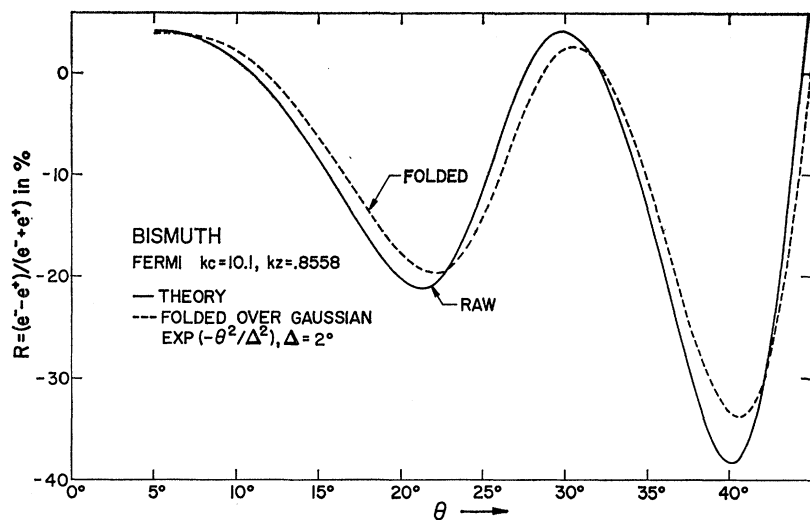


FIG. 4. An illustration of the effect of folding, to allow for the angular resolution of the GPY experiment. The method of folding is described in the text.

taken as 2° . This corresponds to a resolution width of 3.3° (full width at half-maximum). The quantitative effect of this folding is displayed in Fig. 4 for one of the Fermi shapes. Because of the folding of individual cross sections, as required by experiment, the effect is not immediately deducible from the unfolded ratio curve.

Calculations for cobalt with the Fermi shape are shown in Fig. 5. The other shapes have not been included because the appropriate parameter values require a new electron-scattering analysis, which we have deferred until new experimental results are avail-

able, as with bismuth. The full curves include the effect of finite angular resolution, with the same assumptions as for bismuth. The shifting of the structure to larger angles, and the consequently simpler appearance of the curve, result from scattering from a smaller nucleus, according to elementary diffraction considerations.

Figure 6 displays the way in which the sensitivity to the shape depends on the angular region examined, and on the incident energy. The close similarity of the Fermi and modified Gaussian curves, and the progressively increasing difference between them and the parabolic

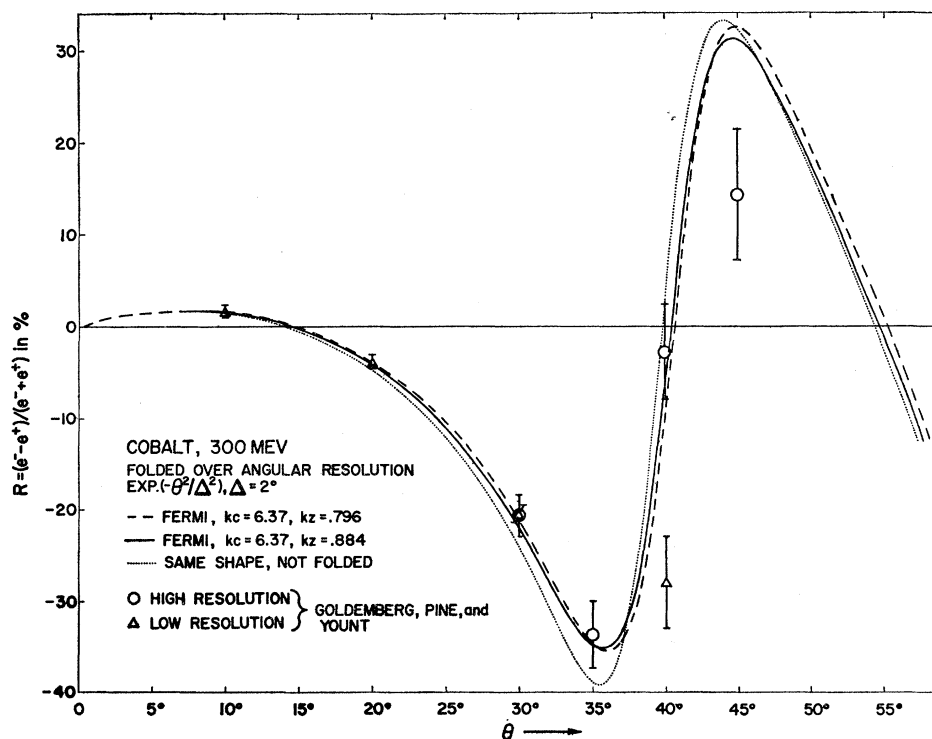


FIG. 5. A comparison of the quantity R expected from the electron scattering analysis (see Ref. 2) and the GYP experiments (see Ref. 1) for cobalt. Only the Fermi shape is considered, because parameter values for the other shapes are not known for the lighter nuclei. The corresponding curves, relative to the Fermi curve, are expected to be similar to those of bismuth, Fig. 3.

Fermi ratio shown in the 300 MeV curves, is an encouraging feature for experimental distinguishability of these shapes, as has been suggested by Rawitscher and Fischer.⁴ It is unfortunately accompanied by the rapid decrease of both electron and positron cross sections to the 10^{-34} cm²/sr range. At this stage even our partial-wave analysis becomes computationally unreliable, which explains why the ratio curves are not given beyond 120°. The 50-MeV curves, which are for the same shapes as the 300-MeV results, but with the parameters kc and kz reduced by a factor 6, have practically no structure, as would be expected from elementary diffraction arguments. The values of R are several times as big as in the corresponding angular region of the 300-MeV curves. This qualitative feature has been noted by Rawitscher and Fischer.⁴ The relative variation in R from one shape to another is however only 50% larger than at 300 MeV, and the cross sections themselves at corresponding values of the recoil momenta are smaller by roughly a factor 30.

IV. DISCUSSION

In over all features the theoretical results obtained for bismuth and for cobalt are very similar, and for each element the characteristic shape of R is rather insensitive to the charge distribution. Some differential cross sections from which R was obtained are shown in Figs. 7 and 8. For each shape and each element, the positron and electron cross sections appear to differ only in being shifted in angular scale. Such a shift can be produced between two electron cross sections either by decreasing the radius or decreasing the energy. The partial-wave analysis is unilluminating as regards such regularity. The second Born approximation method of Drell and Pratt⁸ also sheds little light on it, since the terms neglected in R depend directly on the nuclear charge, and are important even for cobalt. It seems worthwhile to discuss the problem from the point of

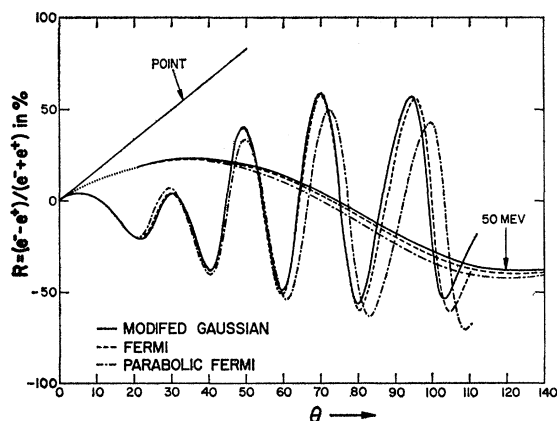


FIG. 6. The quantity R for bismuth, 300 MeV, for the three shapes considered in Fig. 3, plotted over a larger angular range. Also plotted are the corresponding curves at 50-MeV incident energy, i.e., with the length parameters of Fig. 3 reduced by a factor 6. The curves are not folded.

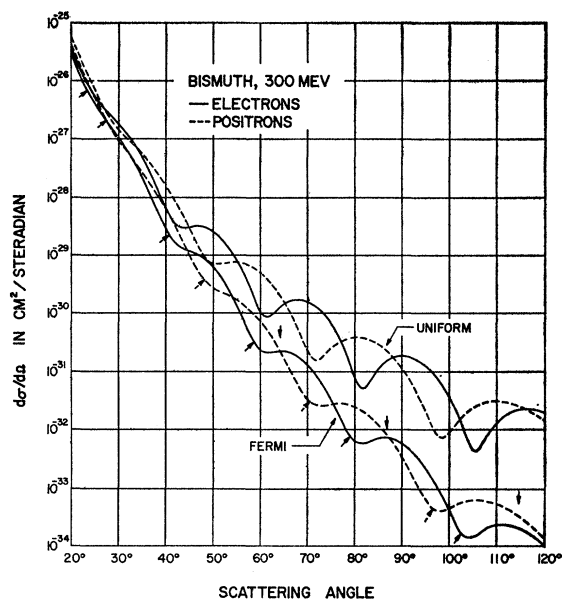


FIG. 7. Differential cross sections at 300 MeV for electrons and positrons on bismuth, for the Fermi shape $kc=10.1$, $kz=0.8558$, and for the uniform shape $kc=10.1$. The vertical arrows indicate the angular positions of the Born-approximation zeros, and the diagonal arrows the shifted positions predicted by the modified Born approximation. The cross sections are not folded over angles.

view of a different approximation, used previously in a similar context by Ravenhall and Yennie.¹⁴ We should reiterate that the results presented in this paper were obtained with the partial-wave analysis and in no way rely on such an approximation.

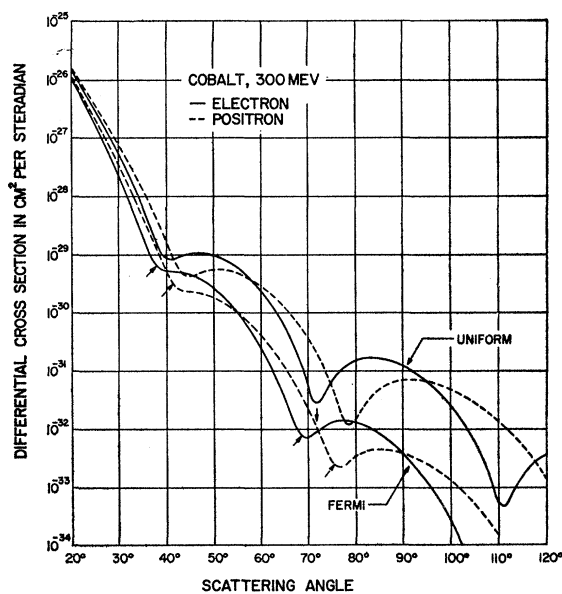


FIG. 8. As for Fig. 7, for cobalt, with the Fermi shape $kc=6.37$, $kz=0.796$, and the uniform shape $kc=6.37$.

¹⁴ D. G. Ravenhall and D. R. Yennie, Proc. Phys. Soc. (London) **A70**, 857 (1957).

The approximation, which seems to predict naturally the above regularities, is a modified Born approximation. For a detailed discussion and justification of its relevance to electron scattering we refer to other papers.^{14,15} Its appealing feature is that the large angle scattering is assumed to arise from one collision, as in the Born approximation. Roughly speaking, the large momentum components of the interaction required to give such large-angle scattering come only from the region of the nucleus. The long-range part of the Coulomb field is very smooth, and does not give rise to scattered waves at large angles. It only modifies the direction and magnitude of the electron momentum at the nucleus. The incident wave function has thus an increased wave number near the nucleus,

$$k(r) = k + (-V(r))/(\hbar c),$$

and has been distorted so that $\mathbf{k}(r)$ is somewhat smeared out in angle about the initial direction of \mathbf{k} . Because of the basic assumption of first Born approximation, the cross sections depend largely on the recoil momentum, or rather, recoil wave number $q = 2k \sin \frac{1}{2}\theta$, apart from the familiar kinematic factors.¹⁶ The above effects on the incident and final wave functions produce a cross section in which the Born approximation appears to have been shifted to smaller angles, because of the increased value of $k(r)$ at the nucleus, and to have been smeared out in angle, because of the smearing of $\mathbf{k}(r)$ in angle. As has been appreciated for a long time, and as appears clearly in Figs. 7 and 8, this is just the behavior exhibited by the partial-wave cross sections. The arrows on the Fermi-shape cross sections show the positions of the Born-approximation zeros, with shifts in angle due to a modification in the wave number of $(\hbar c)^{-1}(\frac{4}{3}Ze^2/c)$. (The quantity Ze^2/c is the value of the Coulomb potential at the half-radius, and the factor $\frac{4}{3}$ gives the average predicted by the approximation).

The implication for *positron* scattering is as follows: The single scattering at the nucleus will be different from that for electrons only because the incoming and outgoing particles have encountered a smooth repulsion instead of an attraction. The effective wave number is reduced, and the wave is diverged rather than converged. The large momentum components caused by the nuclear charge distribution are unchanged however, and the over-all change in sign of the amplitude vanishes on squaring it to get the cross section. The main effect will be to shift the diffraction pattern to larger angles than those of the Born approximation. The smearing effect of $k(r)$ will be more or less the same as for electrons. In Figs. 7 and 8 the positron cross sections obtained by the partial-wave analysis show clearly this effect. To the extent that it is the diffraction structure

produced by the large Fourier components of the Coulomb field which gives information about the nuclear charge distribution, the positron scattering by itself would thus give no more information than has already been obtained by electron scattering. (This holds provided that the interaction is entirely Coulombic.) The possibility that because of the Coulomb repulsion, as compared with the attraction felt by electrons, the positrons will explore differently the various regions of the charge distribution, and so obtain different information about it, would be realized only when the effect of this repulsion on the magnitude of the wave function near the nucleus is appreciable. In bismuth the Coulomb potential is about 20 MeV in the nucleus, and at incident energies comparable with this, the total effect of nuclear finite size on the cross section has become very small. Already at 50 MeV, as is shown in Fig. 6, the variation of R among the various charge distributions is not qualitatively different from that of the corresponding portion of the curve (as regards recoil momenta) at 300 MeV. The quantitative change mentioned in the previous section is largely predicted even by the approximation of Drell and Pratt,³ and does not arise from distortion of the wave function near the nucleus.¹⁷ Thus, at 50 MeV the electron and positron wave functions at the nucleus "see" almost the same thing, and this is much more so at 300 MeV.

The experiment of Goldemberg, Pine, and Yount¹ employs the subtle idea of directly comparing the electron and positron cross sections. Apart from the experimental advantages of such a plan, the theoretical effect is to display a very marked structure, even at small angles. From the cross sections for the Fermi shapes, and for the uniform shapes (zero surface thickness) illustrated in Figs. 7 and 8, it is clear that the effect of smoothing the surface of the charge distribution is to decrease the amplitude of the diffraction wiggles, and also to make the envelope fall off more rapidly with angle. (The angular position of the diffraction structure depends on c , and is not shifted very much. The more rapid decrease is due to the reduction in high-momentum components of the charge distribution, in the modified Born-approximation picture.) The quantity R , which is the difference of cross sections divided by their sum, thus contains the first effect of smoothing the surface, but not the second. This explains the rather low sensitivity to the surface thickness shown in Fig. 2, although the particular form of R , which is restricted to $|R| < 1$, overemphasizes this effect somewhat. The detailed changes among the three Fermi shapes with

¹⁷ With a crude version of the modified Born approximation which contains only the change in wavelength at the nucleus, the quantity R is approximated by $\frac{1}{2}[(\partial F^2(q)/\partial q)/F^2(q)]\Delta q$. Δq is the difference in wave number of electrons and positrons, so that $\Delta q \approx 4(\hbar c)^{-1}(4.3)(Ze^2/c) \sin \frac{1}{2}\theta$. Thus, R is given as a function of q times the kinematic factor $\sin \frac{1}{2}\theta$, which is very similar to the form of Drell and Pratt's³ expression. It is the $\sin \frac{1}{2}\theta$ factor which produces the change in scale of the 50-MeV curves relative to the 300-MeV curves in Fig. 6.

¹⁴ B. Downs, D. G. Ravenhall, and D. R. Yennie, Phys. Rev. **106**, 1285 (1957); D. R. Yennie, F. Boos, D. G. Ravenhall (to be published).

¹⁶ See, for example, R. Hofstadter, Rev. Mod. Phys. **28**, 214 (1956).

varying surface thickness are just what would be expected from these general observations. The effect on differential cross sections of decreasing the radius is to increase the angular scale of the diffraction structure, and thus of R . This is just what is seen in Fig. 2, also. The rather pronounced effect of a central depression in the charge density illustrated in Figs. 3 and 6 is a reflection of the fact that the spacing of the diffraction wiggles varies differently with angle. Whether there is a correspondence of this kind independent of the functional form of the charge density is not known at this stage.

V. CONCLUSION

In bismuth, the range of values of R delimited by the previous electron scattering experiments is exemplified by the curves of Fig. 3, remembering also that each curve has a spread comparable to that illustrated by Fig. 2. The range of values of R in cobalt may be inferred from the bismuth results and the two curves given in Fig. 5. Thus, at 35° the range of values of R allowed by the electron-scattering experiments would be about (-0.35 ± 0.02) , and at 45° $(+0.32 \pm 0.04)$.

The agreement between these predictions and the experimental results of Goldemberg, Pine, and Yount for cobalt is remarkably close. The only disagreement with the high-resolution points of GPY is at 45° , and is less than one standard deviation. The low-resolution points are not able to discriminate against inelastic scattering, which is expected to be most important at the largest angles, and this could explain the 40° low-resolution point. It should be remembered that the

curves are the HRH predictions from electron-scattering alone, and have not been fitted to the GPY experiments. The agreement would presumably be even closer if a mutually best fit were obtained.

Similar remarks apply to the bismuth comparison, Fig. 3. The agreement seems to us very good except for the low-resolution points at small angles, where we do not understand the discrepancy. The curves predicted by electron scattering are model-independent at these small angles, and inelastic contributions to the scattering would be expected to be small. But the over-all agreement between the predictions of the earlier electron scattering experiments of Hahn and Hofstadter, and the electron and positron experiments of Goldemberg, Pine, and Yount, seems to us to be a remarkable confirmation that under the conditions of these experiments, the interaction between electrons or positrons and the nucleus is the static Coulomb interaction. The fact that the ranges of recoil momenta examined by the two sets of experiments were the same prevented the discrimination among possible nuclear shapes which further experiments of either kind at larger recoil momenta will allow. In this regard, the sensitivity of the two kinds of experiment, electron scattering, and the electron-positron scattering ratios, to the features of nuclear charge distributions is somewhat different, and should be allowed for in planning further experiments.

We wish to thank Dr. Goldemberg, Dr. Pine, and Dr. Yount for helpful discussions concerning their experiment, and for their forbearance in holding up their manuscript until our work was ready.